A Brushless Electric Propulsion System for the Research Submersible Alvin

Roger H. Maloof and
Ned C. Forrester

Ocean Engineering Dept.
Woods Hole Oceanographic Inst.
Woods Hole, MA

Charles E. Albrecht

Electric Motion Controls Div.
Moog Inc.
East Aurora, NY

Abstract

Alvin has been fitted with a new propulsion system using multiple thrusters directly driven by brushless electric motors. The high efficiency of direct drive out weighs the use of small thrusters on a large vehicle. Analysis and test data support the improved reliability and performance compared to Alvin's old hydraulic propulsion system.

Introduction

For over twenty years, the 4000 meter research submersible Alvin has been operated and maintained by the Woods Hole Oceanographic Institution. While many substantial improvements were made to the submarine during that time, the original hydraulic propulsion system remained virtually unchanged. During the 1986 overhaul, a new propulsion system was installed, using six thrusters directly driven by 3 hp, brushless, electric motors. The goals for the new system were to improve reliability, maintainability, efficiency, and maneuverability. Another primary goal was to build as much of the new system as possible from commercially available components.

The old propulsion system used a large, steerable stern propeller and two trainable (horizontal to vertical) lift props. These props were driven by hydraulic motors. Hydraulic power was supplied by a pair of 6 hp, brush commutated, DC electric motors driving variable displacement hydraulic pumps. To reduce weight, the hydraulic plant and valving, including the electric motors, were pressure compensated in oil.

Brushes and commutators experience severe carbon build-up and subsequent wear when operated in oil at high pressures. The problem is aggravated by high power operation and Alvin's increased depth limit (a new personnel shpere in the 1970's increased the depth limit from about 2000 to 4000 meters). Even with operational power limits on deep dives, motor overhauls had

Presented at IEEE/MTS Oceans '86, Washington D.C., Manned Vehicles session, Sept. 23-25, 1986.

become frequent.

The primary reason to replace the old propulsion system was that replacements for Alvin's electric motors are no longer available. Other reasons include:

- Maintainence of the tightly packed hydraulic plant was time consuming, requiring that much plumbing be disturbed to reach failing components.
- Efficiency of the hydraulic pumps, motors, valves, and piping was very low.
- Manuverability was limited by the need to steer the stern prop to change its thrust direction.

Propulsion Theory and Practice [1]

The primary task of the propulsion system is to provide the motive force to overcome the hydrodynamic resistive force imposed on the vehicle as it maneuvers through the water. This drag force (D),

$$D = \frac{C_D \rho A_V}{2} V^2 , \qquad (1)$$

is proportional to the square of the vehicle's velocity (V) by its effective drag area ($C_D A_V$) and will require a thrust force of equal magnitude and opposite direction. The thrust produced by a propeller is a function of the net change in momentum of the fluid that passes through it,

$$T = \rho A_T V_J (V_J - V) , \qquad (2)$$

where the area of the thruster (A_T) is the area of the jet of fluid beyond the outlet of the propeller, and the jet velocity (V_J) is the outlet velocity, relative to the propeller. The power required to drive the vehicle (VHP_r) at a given velocity,

$$VHP_r = D V = \frac{C_D \rho A_V}{2} V^3 , \qquad (3)$$

is proportional to the vehicle velocity cubed. Thus to double a vehicle's velocity will require four times the thrust and eight times the power. These hydrodynamic facts are sobering for anyone thinking of drastically increasing a given vessel's speed.

A more realistic goal is to conserve power at a given speed. This can be done by improving the conversions of energy from the power source (batteries in Alvin) to the vehicle. The

conversions are usually compared by the ratio of their outlet to inlet powers. These efficiencies, being multiplicative and not additive, impose great penalties on the overall system by any wasteful conversions along the path.

The hydrodynamic efficiencies can be lumped into one single efficiency,

$$EFF_{PROP} = \frac{VHP_d}{PHP} = \frac{T\ V}{PHP} \ . \qquad (4)$$

The upper power is delivered to the vehicle by the propeller in the form of thrust times velocity (at terminal velocity, $VHP_d = VHP_r$ because T = D). The lower power is the propeller power (PHP),

$$PHP = \frac{\rho\ A_T\ V_J}{2} (V_J^2 - V_A^2) \ , \qquad (5)$$

that the propeller used to produce the change in momentum of the fluid that provides the thrust (T). The velocity of advance (V_A) is the inlet velocity to the propeller, relative to the propeller. V_A is usually slower than the vehicle velocity (V), having been reduced by skin and form drag, dependent on the vehicle geometry.

Thus, substituting (2) and (5) in (4), the propulsive efficiency becomes:

$$EFF_{PROP} = \frac{2\ (\frac{V_J}{V} - 1\ )}{(\frac{V_J}{V})^2 - (\frac{V_A}{V})^2} \ . \qquad (6)$$

An interesting and simple form of the propulsive efficiency occurs when V_A equals the vehicle velocity (V):

$$EFF_{PROP} \Big|_{V_A = V} = \frac{2}{1 + \frac{V_J}{V}} \ . \qquad (7)$$

In this case the efficiency is a function only of the ratio of the exit velocity of the propeller (V_J) to the vehicle velocity (V). The equation shows that the closer V_J comes to V, the greater the efficiency. However, the thrust equation (2) shows that the greatest thrust for a given propeller comes from the

largest difference between V_J and V. In the extreme, when the efficiency is one, the thrust is zero. The only way to get large efficiencies, then, is to increase the propeller area to quite large values.

The compromise between unrealistic propeller size (high efficiency) and small, easily placed propeller size (low efficiency) can be further analyzed by putting the propulsive efficiency in terms of the vehicle's parameters. This can be done by solving for $V_J = f(V)$ at the terminal velocity (vehicle not accelerating) by setting thrust equal to drag. Equating (1) and (2), we find that V_J is proportional to V:

$$\frac{V_J}{V} = \frac{1}{2} + \frac{1}{2}\left(1 + \frac{2\ C_D\ A_V}{A_T}\right)^{1/2} . \qquad (8)$$

Combining (8) with (7):

$$EFF_{PROP}\Big|_{V_A = V} = \frac{4}{3 + \left(1 + 2\ \frac{C_D\ A_V}{A_T}\right)^{1/2}} . \qquad (9)$$

This interesting equation shows that the propulsive efficiency is a function of the square root of the the ratio between the thruster area (A_T) and the vehicle effective drag area ($C_D\ A_V$). In real terms then, the compromise becomes one of either reducing vehicle effective drag area or increasing the total thruster area (one large or many small).

A plot of equation (9) is shown as the curve labled "$V_A/V=1.0$" in Figure 1. The remaining curves in the family show the influence that a reduced inlet flow to the thruster ($V_A < V$) produces. The most obvious change from the ideal curve, $V_A/V = 1.0$, is that the maximum efficiency is reduced to a value less than 1.0, and that this maximum is obtained at a realistic value of A_T/C_DA_V (thruster size near vehicle size), making it possible to optimize the thruster to the vehicle. The other significant effect of reduced V_A is the rapid loss of maximum efficiency with very small reductions to the inlet velocity.

For the geometry of a typical work submersible, the velocity disturbances around the hull are such that V_A/V will be at least 0.9 and probably more like 0.8. The obvious solution is to place the thruster outside this disturbance, but this would cause vehicle enlargement problems and would risk thruster damage due to inevitable collisions in transit and at the work site. Such placement would also cause problems with vehicle launch and recovery.

Another common measure of thruster utility is the production

of static thrust. Static conditions are defined as $V_A = V = 0$. High maneuverability is a function of acceleration (at low speeds) and the ability to command that acceleration promptly. While any thruster can produce any thrust (assuming no cavitation), it can be seen by eliminating V_J from (2) and (5) that the power to produce a given static thrust increases as the size of the thruster decreases:

$$PHP_{static} = \frac{T^{3/2}}{2\ (\rho\ A_T)^{1/2}} \ . \qquad (10)$$

Practical Considerations

The practical limit of propulsive efficiency with Alvin's exsiting profile (low V_A, $C_D A_V = 50\ ft^2$) can be seen from Figure 1 to be about 60%. The old stern propeller ($A_T = 10\ ft^2$) was matched fairly well for these conditions. To reduce the development cost for the new system, an industry standard thruster was chosen; the model 1001 from Innerspace Corp., Covina, CA. Unfortunately, its thrust area is low compared to Alvin's size, requiring high exit velocities. To overcome this, multiple thrusters were aligned with the primary axes of motion. The use of multiple thrusters also aids the goal of increased mission reliability by providing redundancy. Future development might increase the thruster diameter, allowing a possible 20% increase in the propulsive efficiency.

With the decision to use multiple thrusters came the difficult choice of placement, orientation, and possible changes to orientation to reduce the necessary number of thrusters. The more thrusters used, the greater the total weight (including mounts, motors and controllers) and overall electrical complexity.

From discussions with the pilots, the primary axes and the required thrust in each was determined. Alvin's usage is primarily for scientific investigation at sites of known interest; a mission placing emphasis on maneuverability at the expense of top speed. The required maneuvers are: travel along the longitudinal (fore/aft) and the vertical axes, and rotation about the yaw axis (heading). Based on experience with the old propulsion system, longitudinal thrust was considered adequate (visibility and stopping distance limited speed), but more vertical thrust was desired. Heading rate was not critical.

In order to avoid an aborted mission, the design had to provide the required maneuvers given a single failure at almost any point in the propulsion system from the control stick to the thrusters. To furnish this necessitated at least two thrusters able to point in either of the key axes and two means to change heading. In addition, the pilots wanted the ability to produce

high vertical thrust at times (to jump over obstacles, or ascend/decend quickly) and to produce high longitudinal thrust for transit or to buck currents. Luckily, these last two requirements did not have to be satisfied simultaneously. Finally, it was thought that the ability to move laterally while at the work site would be useful; redundancy was not required for this maneuver.

Thruster Arrangement

The new arrangement is shown in Figure 2. Two lift thrusters provide redundant vertical thrust plus lateral thrust. To provide lateral thrust and protect the lift thrusters from damage (by allowing recessed mounting), the thrusters are inclined 30 degrees inboard at the top. Lateral thrust requires the two thrusters to operate differentially (one thrusting up, one down). The vertical vectors cancel and the horizontal vectors add to the equivalent of one "unit" thruster, laterally.

Longitudinal thrust is provided by at least the one fixed thruster mounted centrally aft. Steerage is normally provided by a transverse oriented, aft mounted thruster; this provides a long moment arm for quick and strong heading changes.

To provide high thrust either vertically or longitudinally, two thrusters aft can rotate between these axes, adding to the fixed thrusters in either axis. It would be better to place these thrusters nearer to the center of gravity to reduce the pitching moment when directed vertically, but on Alvin they would be too exposed to damage if mounted amid-ships. Normally these thrusters are used longitudinally, but when they are used vertically or if they should fail, the two fixed aft thrusters provide the required maneuverability. Conversely, if the transverse or both fixed aft thrusters fail, the aft trainable thrusters can be turned horizontal and operated differentially to provide steerage and/or longitudinal thrust.

This arrangement, along with the redundant electrical distribution described later, allows Alvin to maneuver and transit given any single and certain multiple failures throughout the propulsion system.

Motor Characteristics

The thrusters used for the new propulsion system are rated for operation up to 20 shaft horse power. However, in a power limited system, it is more efficient (equation 10) to restrict operation to 3 shp. For this thruster, 3 shp is required at about 1500 rpm. The size, efficiency and economics of the electronic controller for a brushless motor required that Alvin's battery voltage be raised from 60 VDC to 120 VDC. Thus, the

basic motor specifications were:

- brushless design,
- 5 inch diameter, minimum length,
- 3 hp output at 1500 rpm,
- operation from 120 VDC bus, nominal, 108 V minimum,
- controller to fit in 7.5 inch ID pressure housing,
- 75% efficiency (motor and controller), at full load.

Although a complete discussion of brushless motors is beyond the scope of this paper, a brief introduction will identify some of the advantages of brushless motors in submerged applications. Although various approaches are taken in designing brushless motor systems, there are several key characteristics that define a brushless motor. Current carrying conductors are wound on the stationary stator with permanent magnet poles attached to the rotor of the brushless motor. This is just the reverse of the more traditional permanent magnet, brush motor. Figure 3 shows a cross sectional comparison of a typical brush and brushless design. For rotation to occur in a motor, the electromagnetic field produced by the windings must be phased or sequenced in some defined fashion with respect to the permanent magnet field. This process is called commutation. Brush designs implement commutation by means of fixed mechanical brushes and a series of radially segmented contacts (commutator) attached to the wound rotor. In a brushless motor, commutation is performed electronically. In order to maintain the proper phasing between the permanent magnets and the electromagnetic fields, brushless motors employ a rotor position sensor for commutation. The brushless motor is "self-synchronous" in that the frequency of excitation to the stator windings is electronically interpreted from the rotor position device.

Brushless motor technology offers the highest power output for a given package size and weight over brush or induction type systems, for several reasons. Heat produced in the motor, mainly due to I^2R losses in the copper winding, has a direct thermal conduction path from the stator through the motor housing to the ambient water. In brush motors, heat losses must be channeled through an additional gas or fluid gap between the rotor and stator.

Alvin's thruster motors use rare earth samarium cobalt, permanent magnets in a high pole count rotor configuration. Samarium cobalt has a high energy product, excellent temperature properties, and does not "rust" in the presence of water contamination. The high number of rotor poles permits high torque from a relatively small rotor diameter. Brushless motors also have superior speed-torque operating ranges that are not limited by brush heating or commutator arcing.

Motor Design

Alvin's thrusters and the accompanying electronic controllers were designed and manufactured by Moog Inc, Electric Motion Controls Division, East Aurora, New York. The housings, cabling and other parts of the motor/controller system were designed by Woods Hole Oceanographic Institution.

An assembled motor is shown in Figure 4. The stator has a 3 phase, sinusoidal back EMF winding with a class F specification that is capable of continuous operation up to 155^{o}C. The stator-rotor envelope is 5.062 inches in diameter by 2 inches deep. The weight of this assembly (exclusive of connecting shaft) is 10.5 lbs.

Rotor feedback for the brushless motors on Alvin is provided by a pancake transmitter style resolver. The resolver is a wound, analog type transducer that outputs two continuous amplitude modulated signals in quadrature. These signals are electronically interpreted to determine motor rotor position for accurate commutation control. The resolver, itself, has no contacting parts (brushless) and contains no electronic devices, making it well suited to high temperature, shock and pressure.

The motor housing is constructed of titanium and PVC plastic for corrosion resistance with an overall length of 12.25 inches and a diameter of 5.365 inches. The small size minimizes interference with the flow of water through the thruster. Wires to the motor are contained in a 3/4 in ID hose; this hose attaches directly to the motor housing to avoid flow interference from a bulky connector. The motor/cable assembly is filled with MIL-H-5606 hydraulic fluid for pressure compensation and lubrication; a small diaphram mounted in the PVC end cap together with the cable hose compensate for compression of the oil and any trapped bubbles. The shaft is sealed with a spring loaded carbon on ceramic seal. The stator and case make a sliding fit at room temperature, but as the motor heats up, the iron stator expands more rapidly than the case, increasing the thermal contact. The total weight of a thruster, motor, attached cable and oil is about 45 lb.

Motor Controller

Each thruster motor is powered by an analog velocity controller. The controller performs speed regulation, electronic commutation control, high power 3 phase inversion, and system protection. Figure 5 illustrates the controller-motor functionality.

The controller is a velocity servo that compares an analog speed command to actual motor speed and generates a correctional error signal if they are different. The motor speed feedback is

electronically derived from the motor resolver position feedback. The velocity servo loop contains a P-I compensator (proportional-integral gain) which facilitates precise speed regulation from no-load to fully loaded shaft torques.

Electronic commutation circuitry processes the rotor shaft position from the resolver to provide accurate phasing of exitation currents to the motor. The commutation output is a 3 phase, balanced sinusoid to match the brushless motor winding design. Commutation phasing maintains an optimum angular relationship between the stator and rotor magnetic vectors so as to produce maximum torque per ampere of motor excitation. The commutation control also processes the velocity loop error signal, providing an amplitude for the 3 phase sinusiods that is proportional to velocity error.

Power from Alvin's 120 volt DC bus is inverted, under direction of the commutation control, to sinusoidal 3 phase currents for producing motor torque. The power stage is a current regulator with pulse width modulated (PWM switch mode) power outputs. Current regulation is accomplished by comparing actual motor phase current to commanded current from the commutation control. The output bipolar transistors are configured in a 3 phase H-bridge. By modulating the relative "on" and "off" times of devices in the bridge, motor current polarity and amplitude are controlled. Device power dissipation in either the on or off state is relatively small, allowing a reasonably sized package to switch significant power to the motor windings.

The PWM switching frequency is held constant. Selection of a PWM switching frequency was based on possible acoustic interference problems. When switching current to the motor, chatacteristic acoustical noise is generated at the base PWM frequency and its harmonics and side-bands. It was first determined that a frequency above 15 kHz would be higher than most navigational equipment. Alvin uses two higher frequency devices; a CTFM (continuous transmission, frequency modulation) scanning sonar which operates in a band from 69.5 kHz to 89.5 kHz, and a 100 kHz narrow band altimiter. The PWM switching frequency was selected at 22.73 kHz to avoid harmonics at these frequencies.

Important to any control system is a way to protect equipment when abnormal or excessive conditions occur. The motor controllers used on Alvin provide built in protection as follows:

Shut down:
- Loss of resolver feedback
- Loss of voltage to control circuits
- Heat sink temperature over $80^{o}C$
- Motor output short circuit

Current limit:
- Peak current output limit

- Excessive current demand over time (I-T)

Loss of resolver feedback, control voltage, over temperature, or any phase-to-phase or phase-to-bus short circuit automatically disables the power outputs, thus preventing unpredictable motor behavior and/or equipment damage. Peak current limiting allows the maximum system current to be set from 10% to 100% of maximum controller output. If excessive current is demanded over a preset time interval, the I-T protection lowers (folds back) the available controller output current to a safe level. Both the time and the fold back current are adjustable.

The motor controllers are packaged as shown in Figure 6. To save weight and space without sacrificing too much redundancy, controllers for two motors are contained in each of four pressure housings. The housings are 17-4 stainless to lower the cost, while the end caps are titanium to save weight. Each housing also contains control power supplies, interface circuits, and power input filtering and protection. A small fan provides efficient heat transfer for the air cooled devices. The housings are purged with Freon to prevent condensation.

Controller efficiency is approximately 90% at full load with Alvin's 120 VDC bus. (The controllers are capable of 95% efficiency when operated at 320 VDC with the corresponding higher motor speed). Thus, at 3 shp from the motor, about 300 watts must be dissipated from each controller's output stage. This heat is conducted through a semi-circular heat sink, through the wall of the pressure housing, to sea water. Heat sink grease is used at all interfaces.

Motor Power Distribution

A simplified electrical distribution system is shown in Figure 7. The batteries are connected to the oil filled control center where power is passed by open frame contactors to two 120 volt relay housings. These relay pressure housings contain motor and lighting vacuum relays from which power is applied to pairs of motor controllers in their own housings. Most motor cables are oil filled hose with pressure balanced connectors; this configruation allows flexibility in selection of wire types and sizes. In addition to the thruster motors, Alvin's variable ballast pump and hydraulic system pump are also driven by the new brushless motors; these pumps are mechanically configured so that either motor can drive either pump, if required.

By using a tree structure and assigning each motor to an appropriate branch of the tree, substantial redundancy is provided. It is clear that the three thrusters assigned to either the top or bottom half of the tree can provide all required maneuvers in the absense of the other half. It is thus also clear that any single failure or flooding of any container

or component will not prevent continuation of a dive. The only exception is flooding of the control center; but, due to oil filling and a leak detector, any leak is expected to be slow and detected promptly. The relays and contactors allow any flooded motor, housing or cable to be isolated from the electrical system to prevent corrosion.

Operator Controls

Thruster motor speed is governed by an analog signal produced in the personnel sphere. Several methods are provided to generate these signals for both convenience and redundancy.

Normal control is from a four axis, "T" handle joystick. Fore/aft motion of the handle controls longitudinal thrust, twist controls steering thrust, left/right motion controls lateral thrust, and a thumb actuated control in the left end of the "T" controls vertical thrust. All axes are spring return to zero. This control is mounted on the right side of the sphere. It is used when temporary inputs are required (normal) and when the pilot must look out the starboard viewport.

Secondary control is provided by four knob controls with center detents and friction hold; they control the same four axes as the joystick and their output is added to that of the joystick. These knobs are used to select steady thrust for "cruise control", to augment the variable ballast system, to hold Alvin in a particular crack while sampling, etc. Addition with the joystick outputs allows a bias to be set with the knobs while normal control is still possible from the joystick. These controls are mounted on the left side of the sphere and are used when the pilot needs to look out the port viewport.

Auxiliary controls are located in the sail (conning tower) for surface maneuvering. These are simply two water proof, double throw, center off switches that apply full ahead or reverse power to the aft thrusters for transit and steering.

For backup, a very simple control system consisting of a double throw switch for each thruster is provided on the port side of the shpere. This system includes a three speed switch to control the magnitude of the thrust impulses provided by the switches.

Each motor controller returns status to the sphere. The signal is coded with a pulse for each revolution of the motor to present a blinking light that confirms motor operation and speed to the pilot. The signal is further coded to provide direction information for this motor speed. This signed speed may be displayed on the pilots video screen and logged at intervals on disk. Any fault detected by the controller is indicated by forcing the status signal to a steady on state.

Motor and Thruster Test Results

The motor/controller was tested on a dynamometer. Figure 8 shows the maximum operating envelope of the motor with a 108 VDC supply (Alvin's minimum bus voltage) and no windage or friction. Continuous operation in water is possible anywhere under the curve. Higher voltages allow an increase in the maximum speed. Maximum power available is over 4 hp at the knee of the curve. Efficiency was checked at 1480 rpm and 136 lb-in (actual output torque, with seal and oil) with a DC bus current of 30.2 amps at 108 volts; the overall efficiency was 73%, or 76% for the motor not counting the friction.

Friction and windage were measured at various speeds on the dynamometer with seal and oil installed and no excitation of the motor. The seal produced a static 3.5 lb-in torque at low speed. The total friction rose linearly with speed to 7.5 lb-in at 2500 rpm. This is plotted in Figure 8. The linear rise suggests that the windage loss in the oil is due to shear rather than turbulence. The oil temperature was approximately 50°C during this test.

The thruster and motor were mated and suspended vertically from a scale in 6 to 8 feet of sea water. Thrust, motor speed, motor phase current and DC bus power were measured at various speeds. Shaft torque was calculated from phase current and motor speed as calibrated on the dynamometer. As expected from theory, the data show that both thrust (T) and torque (Q) are functions of the square of the shaft speed (n). Linear regression yeilds a best estimate of T (lb) and Q (lb-in) in both ahead and reverse directions as a function of n^2 (rpm^2):

$$T_A = 158 \left(\frac{n}{1500}\right)^2, \quad T_R = 131 \left(\frac{n}{1500}\right)^2, \text{ (lb)} \qquad (11)$$

$$Q_A = 112 \left(\frac{n}{1500}\right)^2, \quad Q_R = 132 \left(\frac{n}{1500}\right)^2. \text{ (lb-in)} \qquad (12)$$

Reverse torque may be too high based on some over estimation of motor torque in this direction. These measurements were made without filling the motor mounting bolt recesses in the thruster; Innerspace recommends filling the recesses. Equation (12) is plotted on Figure 8 to show the matching of the thruster and motor.

The required shaft horse power can be calulated from the torque:

$$SHP_A = 2.67 \left(\frac{n}{1500}\right)^3, \quad \text{(hp)} \qquad (13)$$

The propeller power (10) is the axial kinetic energy added to the thruster outlet jet. The actual shaft horse power is greater than this due to various losses in the action of the thruster. From equations (10), (11) and (13), the efficiency of the thruster as a water pump (EFF_T) can be found,

$$EFF_T = \frac{PHP}{SHP} = \frac{T^{3/2}}{2\ C\ SHP\ (\rho\ A_T)^{1/2}} = .57\ , \qquad (14)$$

for the ahead direction, based on a thruster outlet area of 0.721 ft^2 (C = 550 ft-lb/sec/hp).

A temperature sensor was installed on the stator winding of the motor. The thruster was operated continuously in sea water at 1550 rpm. The temperature rise of the winding was limited to about 20°C and showed a 5 minute time constant.

Temperature rise in the controller housing was tested in still sea water (in a tank) with one controller operating at full load. One temperature sensor was placed between two of the horizontally oriented controller circuit boards, and another was placed on the controller base plate near a power transistor. With no fan running and no heat sink grease between the semi-circular heat sink and the pressure housing, temperature rise between the boards was over 65°C and on the base plate 41°C. With the fan running the temperature rises were 30°C and 34°C, respectively. When heat sink grease was added between the heat sink and the housing the temperature rise of the base plate was only 25°C. With heat sink grease, the base plate showed about a 7 minute time constant.

A controller, motor and thruster were operated continuously for about 15 days at varying speeds. During this interval about 40,000 power on/off cycles were performed. Only one controller failure occurred during this test.

All thruster motors were pressure tested to 9000 psi for one cycle with no failures. One motor was spun without load during a ten cycle test. By monitoring the controller input power, a measure of the friction load on the motor was obtained. At 2100 rpm, the input power increased by about 50% when the pressure changed from zero to 9000 psi. Subtracting the seal friction, this would indicate that the windage torque due to oil drag approximately doubled.

Bollard pull tests were conducted on Alvin in both longitudinal and vertical directions with several combinations of thrusters. The data were quite variable due to the difficulty of

obtaining an average scale reading in the light surge near the dock. However, the single thruster data was generally confirmed. The principle exception was aft thrust; it appears that the slope of Alvin's skin and interference of the fenders on the aft trainable thrusters (not shown in Figure 2) significantly deflect the outlet jet. Aft thrust was about 30% less than predicted by equation (11).

Comparison of Old and New Propulsion Systems

Performance data from the original Alvin was reported by Mavor, et al. [2] in 1966. Maximum static thrust for the stern propeller was about 300 lb ahead and about 230 lb reverse. Using three thrusters at 1600 rpm, the new system provides 540 lb ahead and 310 lb reverse.

The old lift props provided 200 lb and could be rotated up or down. The new system provides 310 lb up and 260 lb down with two thrusters, or 670 lb up and 550 lb down with all four thrusters. This provides the substantial lift improvement that was desired.

Mavor lists the efficiency of the hydraulic plant components as shown in Figure 9. The efficiency from battery to shaft is only 26.7%. The efficiency of the propeller may be calculated from (13) and the data point of 285 lb thrust generated from 5 kW; the diameter of the outlet jet is assumed to be 85% of the 50 inch diameter propeller, giving A_T = 9.85 ft^2. The resulting EFF_T is 56%. The propulsive efficiency is found from (6) and (8), assuming low V_A, to be 50%. The overall propulsive efficiency is only 7.5%.

For the new system, (see Figure 9) the conversion efficiency from battery to shaft is greatly improved, at 75%; this improvement is the prime reason for the overall advantage of the direct drive electric system. The thruster efficiency was given in (13). The propulsive efficiency calculated as above is only 38%, but is more than compensated by the improved conversion efficiency. The overall propulsive efficiency is 16.4%, more than twice the old system. The new system is also capable of using more battery power without depth limitations, so that the total power available to propel Alvin is more than 3 times greater, yeilding a possible top speed increase of 50%.

To compare the efficiency of static thrust production between the old and new systems, use equation (10) with the same thrust for both systems, along with the conversion and thruster efficiencies:

$$\frac{P_O}{P_N} = \frac{A_{TN}^{1/2}\ EFF_{TN}\ EFF_{CN}}{A_{TO}^{1/2}\ EFF_{TO}\ EFF_{CO}},$$

$$\frac{P_O}{P_N} = \frac{(2.16)^{1/2} \times .57 \times .76}{(9.85)^{1/2} \times .56 \times .27} = 1.3$$

The old system uses 30% more power to create the same thrust, but the new system is heavily penalized for its small thrusters because the square root of the area ratio is a direct factor in this comparison.

Conclusions

Performance of the new propulsion system has been excellent on 65 dives so far this year. During harbor trials, a contaminated connector caused a motor output short circuit; the controller detected this and shutdown without damage. Thrusters have been stalled twice and the redundancy has allowed the dives to continue without notice. Reliabilty has already surpassed that of the old system; there have been no failures other than those caused by external events. The first challenging mission for the new system was the Titanic visit. Heavy currents and scattered debris demanded precision piloting and immediate response from the thrusters. The crew reported superior control and maneuverability, and doubted whether the old system could have done half the mission. To quote the cheif pilot, "It drives like a sports car."

Future work on the propulsion system will be aimed at reducing the size of the controllers and simplifying or eliminating the cabling between motors and controllers.

Acknowledgements

This work was supported by grants from the National Science Foundation, OCE-8320508, OCE-8316583 and additional support from the Office of Naval Research, the National Oceanic and Atmosphereic Administration and the National Science Foundation through NSF grant OCE-8214507.

References

[1] Principles of Naval Architecture, SNAME, 1967, pp. 370-462.

[2] Mavor, James W., Jr., et al., "Alvin, 6000-ft Submergence Research Vehicle", SNAME, Transactions, 1966, p. 106.

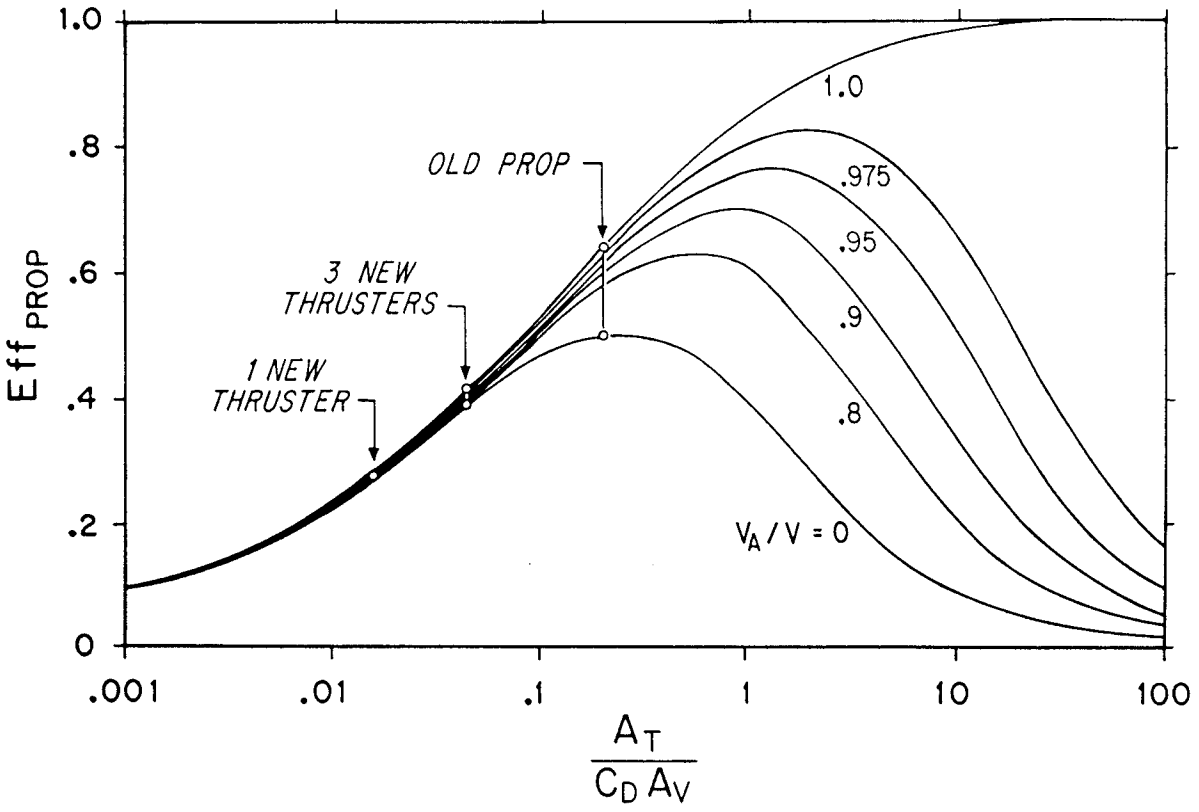

PROPULSIVE EFFICIENCIES

FIGURE 1

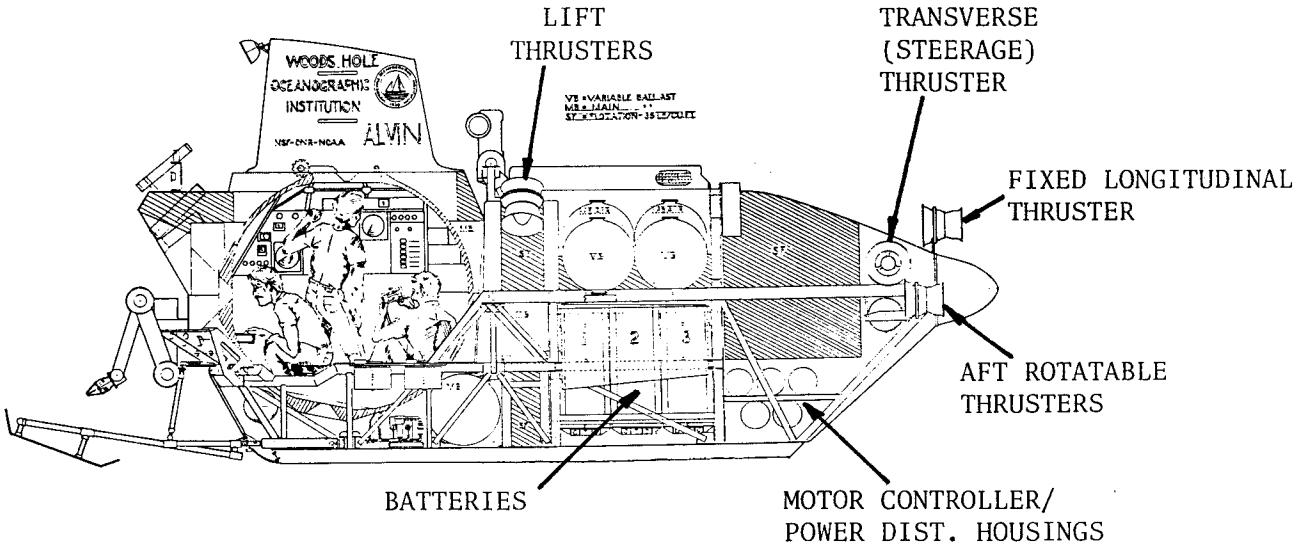

FIGURE 2- ALVIN INBOARD PROFILE

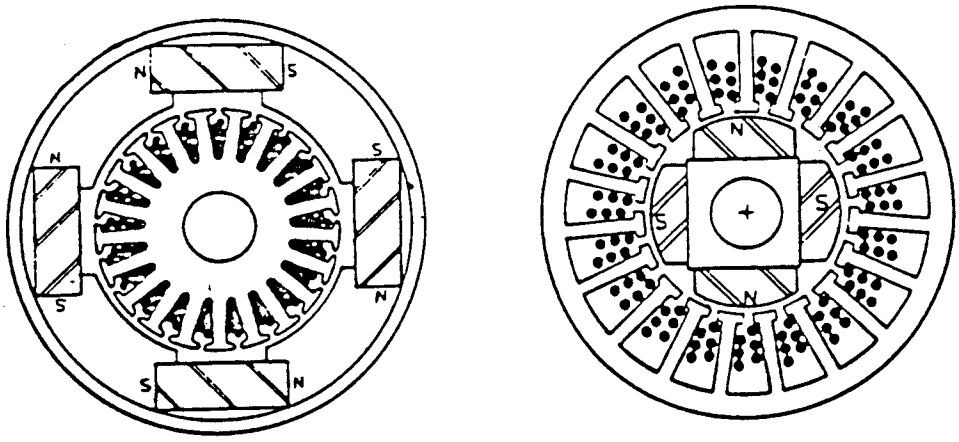

WOUND ROTOR DESIGN
(Brush Type)

WOUND STATOR DESIGN
(Brushless Type)

MOTOR STRUCTURES

FIGURE 3

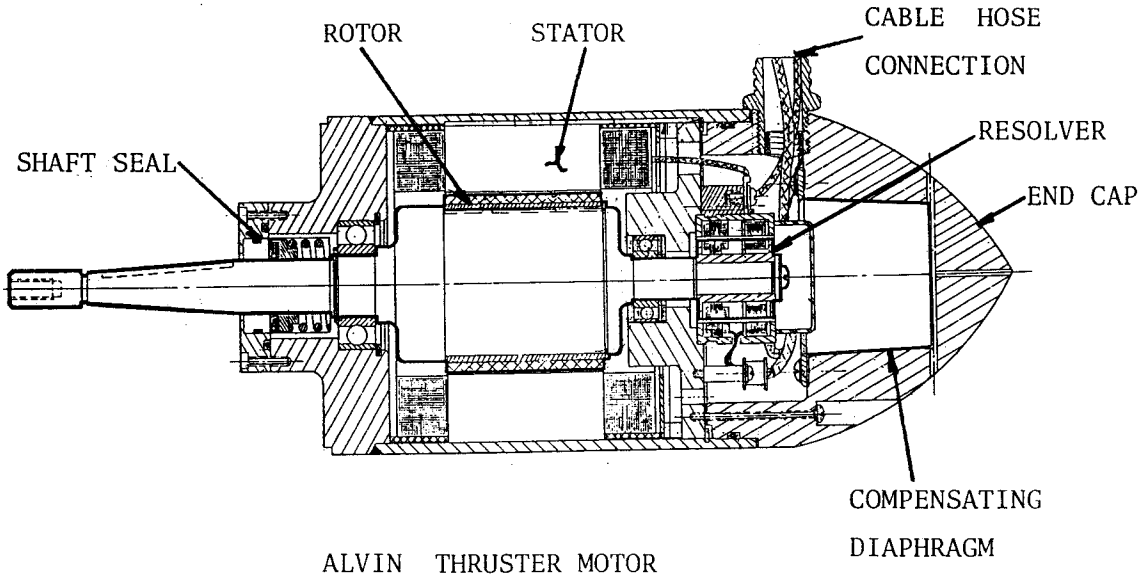

ALVIN THRUSTER MOTOR

FIGURE 4

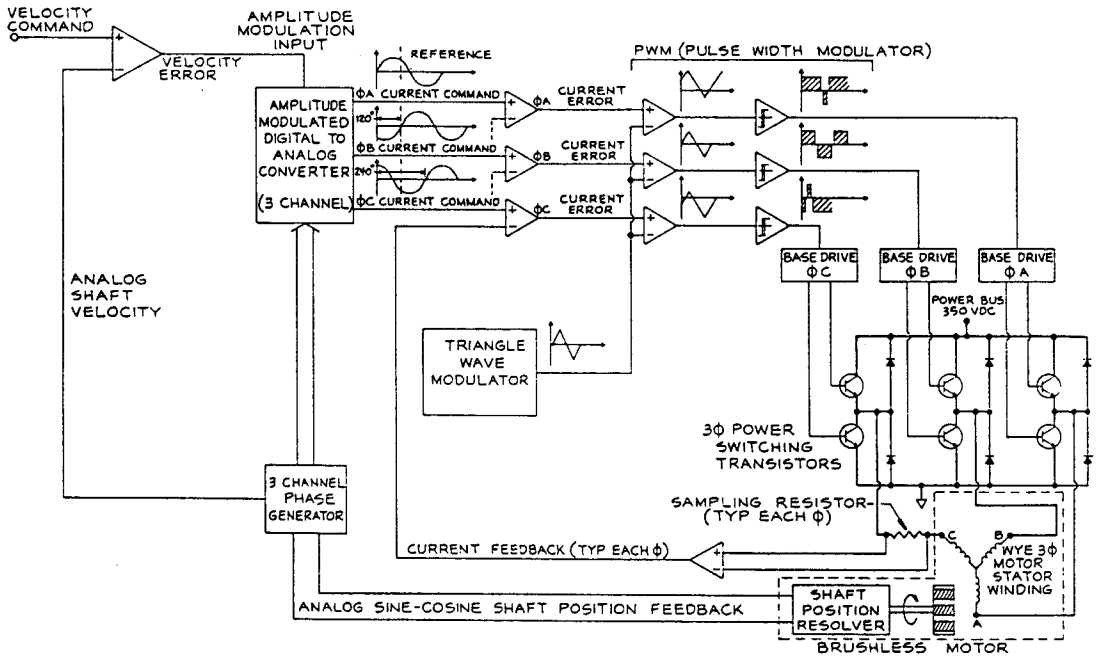

CONTROLLER DIAGRAM

FIGURE 5

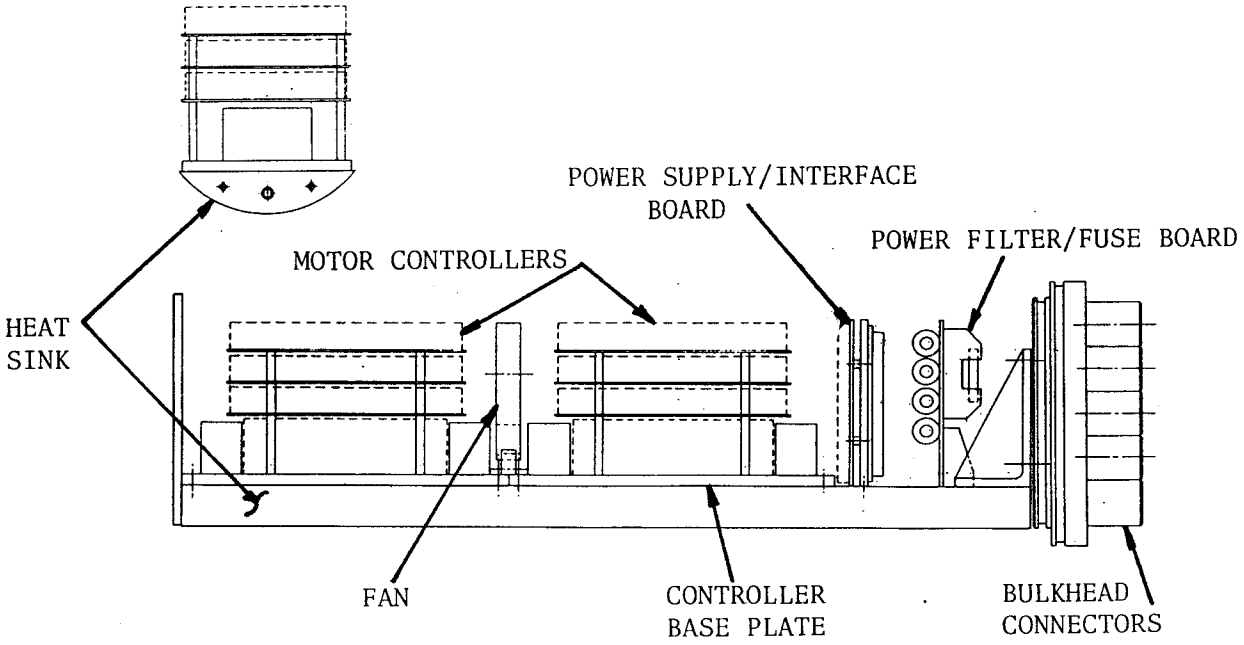

FIGURE 6 - MOTOR CONTROLLER HOUSING

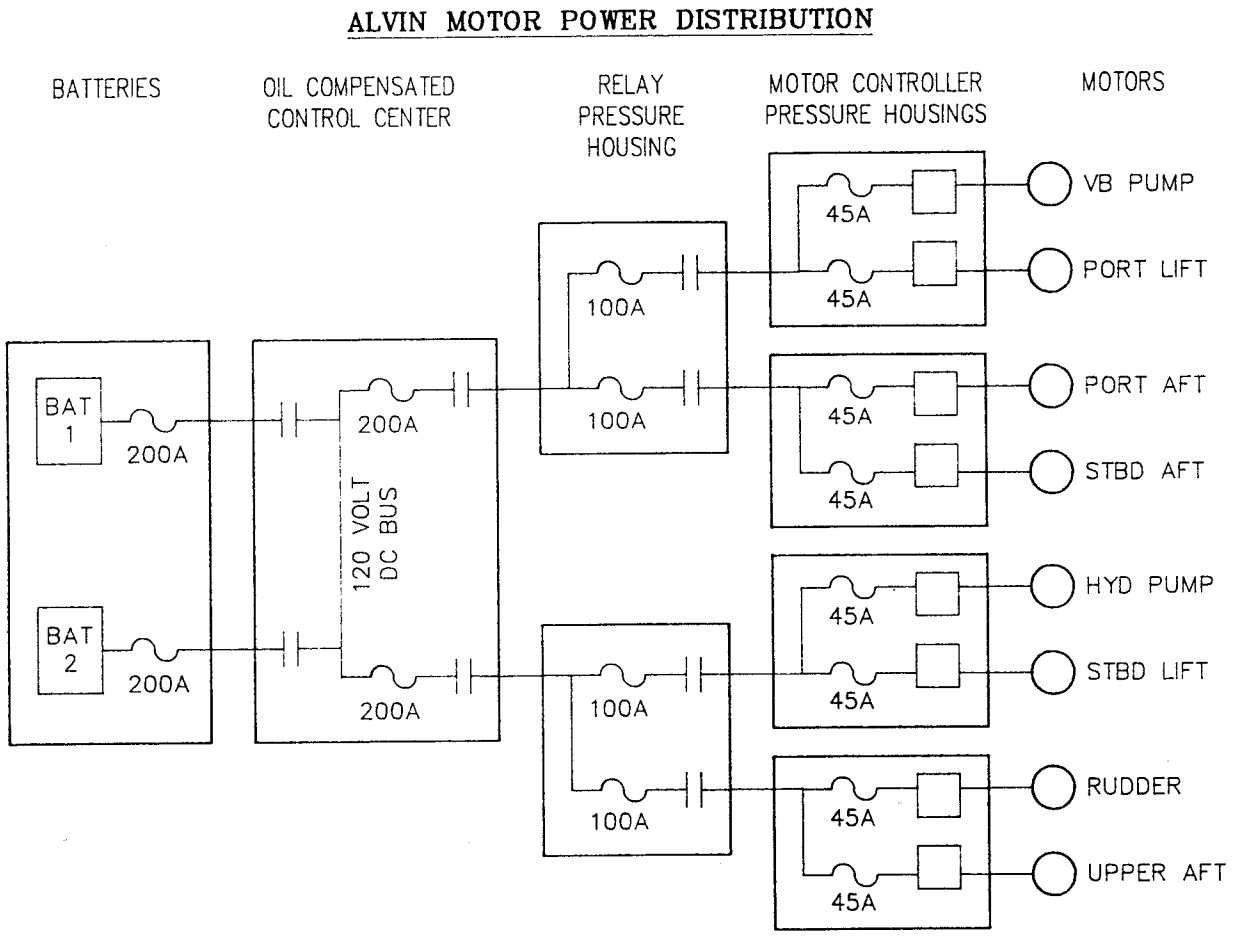
ALVIN MOTOR POWER DISTRIBUTION
BATTERIES
OIL COMPENSATED CONTROL CENTER
RELAY PRESSURE HOUSING
MOTOR CONTROLLER PRESSURE HOUSINGS
MOTORS
BAT 1
200A
BAT 2
200A
200A
120 VOLT DC BUS
200A
100A
100A
100A
100A
45A
45A
45A
45A
45A
45A
VB PUMP
PORT LIFT
PORT AFT
STBD AFT
HYD PUMP
STBD LIFT
RUDDER
UPPER AFT

FIGURE 7

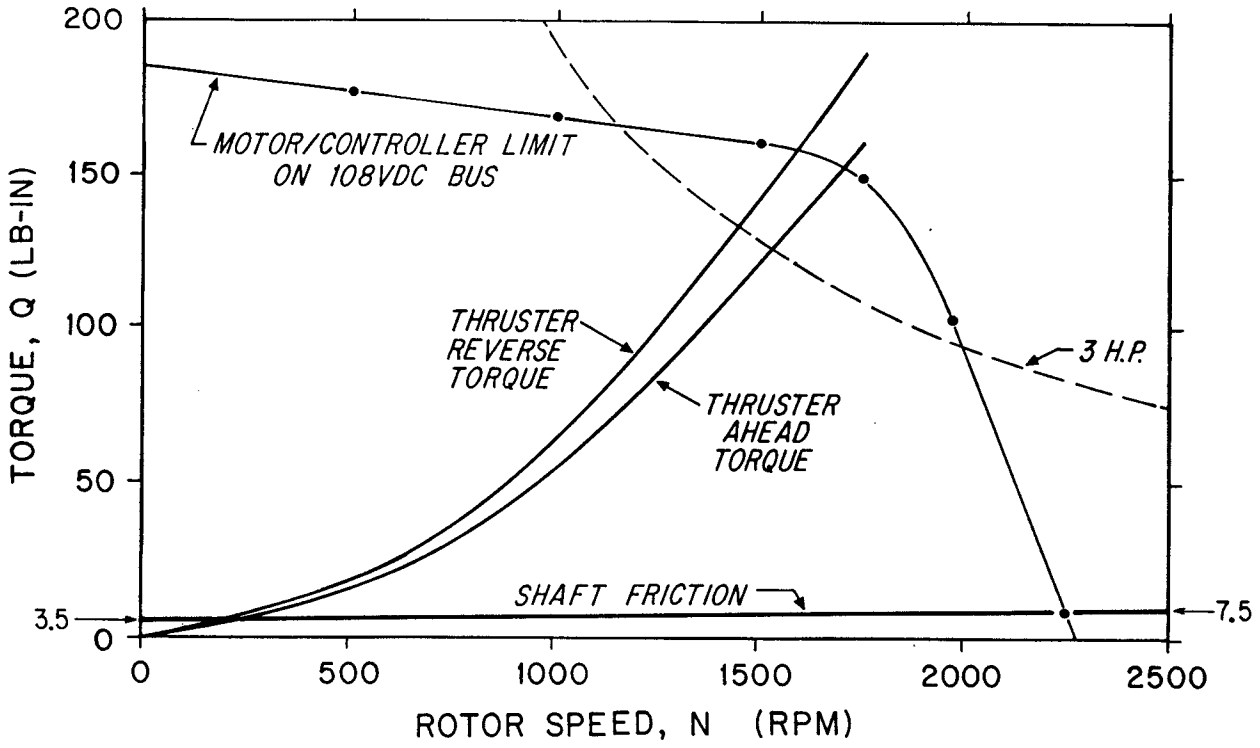

FIGURE 8 - MOTOR/THRUSTER SPEED/TORQUE CURVES

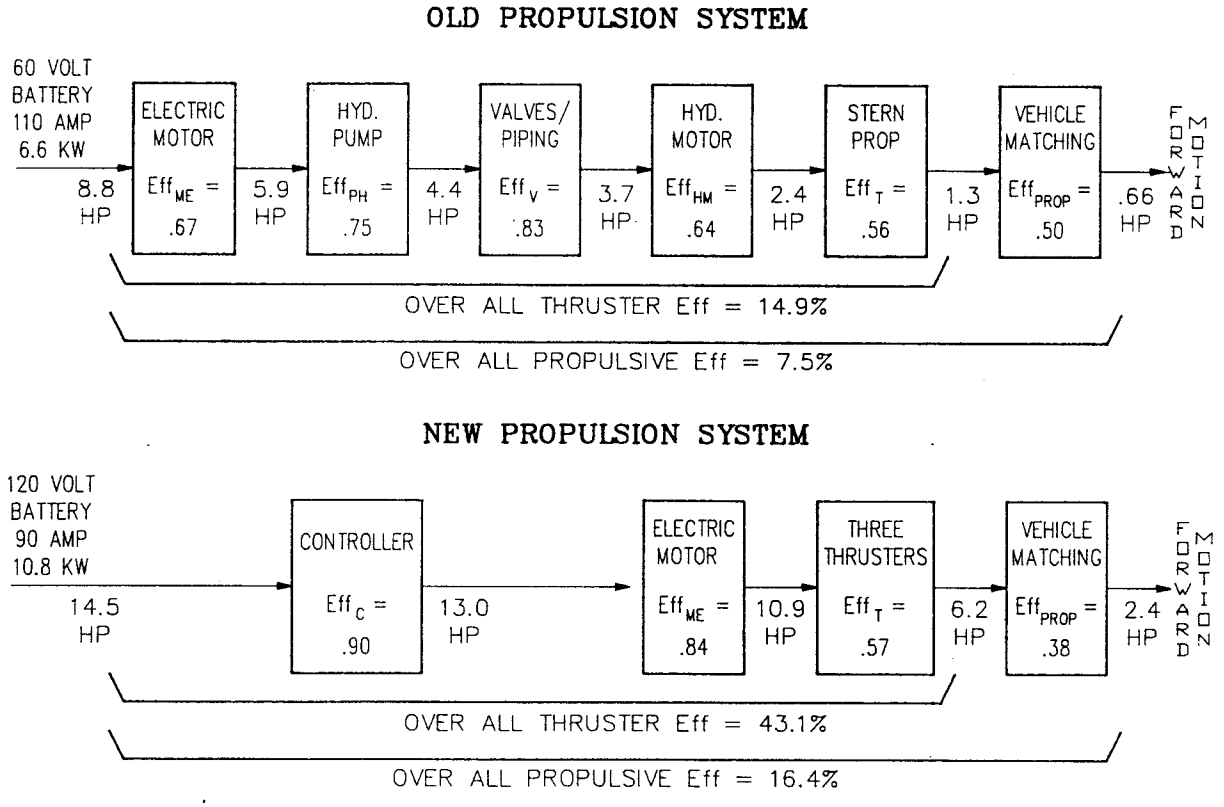

FIGURE 9 - EFFICIENCY COMPARISION